

## Field Stack in Minutes: No Velocity Picking, No Nmo Stretch

Brodic, Bojan ; Papadopoulou, M. ; Draganov, D.S.; Malehmir, Alireza

**DOI**

[10.3997/2214-4609.202220054](https://doi.org/10.3997/2214-4609.202220054)

**Publication date**

2022

**Document Version**

Final published version

**Published in**

28th European Meeting of Environmental and Engineering Geophysics

**Citation (APA)**

Brodic, B., Papadopoulou, M., Draganov, D. S., & Malehmir, A. (2022). Field Stack in Minutes: No Velocity Picking, No Nmo Stretch. In *28th European Meeting of Environmental and Engineering Geophysics*  
<https://doi.org/10.3997/2214-4609.202220054>

**Important note**

To cite this publication, please use the final published version (if applicable).  
Please check the document version above.

**Copyright**

Other than for strictly personal use, it is not permitted to download, forward or distribute the text or part of it, without the consent of the author(s) and/or copyright holder(s), unless the work is under an open content license such as Creative Commons.

**Takedown policy**

Please contact us and provide details if you believe this document breaches copyrights.  
We will remove access to the work immediately and investigate your claim.

***Green Open Access added to TU Delft Institutional Repository***

***'You share, we take care!' - Taverne project***

**<https://www.openaccess.nl/en/you-share-we-take-care>**

Otherwise as indicated in the copyright section: the publisher is the copyright holder of this work and the author uses the Dutch legislation to make this work public.

## FIELD STACK IN MINUTES: NO VELOCITY PICKING, NO NMO STRETCH

B. Brodic<sup>1,2</sup>, M. Papadopoulou<sup>1</sup>, D. Draganov<sup>3</sup>, A. Malehmir<sup>1</sup>

<sup>1</sup> Uppsala University; <sup>2</sup> Geological Survey of Finland; <sup>3</sup> Delft University of Technology

### Summary

---

Motivated by the ideas of automatic common-midpoint (CMP) stacking without normal-moveout (NMO) correction, hence NMO stretch, and automatizing the velocity model building, we propose a cross-correlation/cross-coherence-based approach. It is a two-step method where the first step is cross-correlation/cross-coherence of zero-offset traces with all other traces in corresponding CMP gathers. This step removes the NMO effect of different hyperbolic events, resulting in CMP gathers with flat events without any stretching effect. Following this, horizontal summation across different CMP gathers is done, resulting in a velocity-free data-driven production of time-domain stacked seismic section. The second step takes advantage of the cross-correlation lags via data-driven k-means cluster analysis to separate lags corresponding to individual hyperbolic events in the CMP gather into distinct clusters. Different norm fittings to lags within individual clusters are evaluated and the lowest residual one automatically selected, resulting in a velocity and zero-offset two-way traveltime time per cluster. These form a base to build an average velocity model for migration and time-to-depth conversion. We demonstrate the efficiency of the proposed method using synthetic and field shear-wave data acquired in southwestern Sweden.

## Introduction

Reflection seismic data processing is a challenging task depending on factors such as favorable signal-to-noise ratio (SNR), proper selection of individual processing steps and velocity model building, among others. The two most used approaches for reflection seismic data handling involve conventional CMP processing and prestack depth/time migration, both having in common a velocity model. The CMP processing relies on the hyperbolic nature of events in the CMP gathers, where the velocity model is firstly used for NMO corrections to flatten the events. An inherent part of the NMO process is the NMO stretch effect requiring a careful selection of the stretch mute percentage to avoid degradation of the final stack, particularity for shallow and large offset events (Barnes, 1992). To avoid this effect, different non-stretch NMO corrections have been proposed (i.e., Perroud and Tygel (2004); Biondi et al. (2014); Sheng et al. (2022) and references therein).

Recently, Qiao et al. (2021) and Liang et al. (2022), proposed an approach for NMO corrections based on cross-correlation. We extend this approach to remove the NMO effect and via k-means clustering, we obtain an average velocity model. The latter is used for migration and time-to-depth conversion.

## Automatic NMO corrections

Following Harmankaya et al. (2013) and Kaslilar et al. (2014), and according to Qiao et al. (2021), the proposed method uses cross-correlation/cross-coherence to remove the portions of the seismic wavefield between surface sources and receivers and subsurface reflectors.

For the ease of explanation, we assume sources and receivers located at the free surface of an attenuation-free, noise-free, homogeneous and isotropic media with a horizontal interface at depth and the only recorded arrival in a CMP gather being a reflection from the interface. Cross-correlation of the zero-offset trace with all other traces will yield a CMP gather where times are reduced by the two-way traveltime from the surface to the reflector. In the frequency domain, a trace with reduced time after cross-correlation  $Rcc_{m-t0}(\omega)$  is

$$Rcc_{m-t0}(\omega) = S_m(\omega) S_{t0}(\omega)^*,$$

where  $*$  denotes complex conjugate,  $S_{t0}(\omega)$  – the recorded zero-offset wavefield, and  $S_m(\omega)$  – the reflection time at the  $n$ -th receiver. Cross-correlating the  $Rcc_{m-t0}(\omega)$  traces with the original ones, the time difference between the zero-offset reflection arrival time and the NMO shifts is removed. The NMO-corrected wavefield at the  $n$ -th receiver after cross-correlation -  $CcNMO_m$  – is

$$CcNMO_m(\omega) = S_m(\omega) Rcc_{m-t0}(\omega)^*.$$

To suppress additional wavelet lobes inherently introduced by the cross-correlation, and provide an alternative to handling low SNR data, we also apply cross-coherence as in Place et al. (2019). The cross-coherence-based NMO-corrected wavefield at the  $n$ -th receiver, with  $Rch_{m-t0}(\omega)$  being the reduced reflection time after cross-coherence, is given by

$$ChNMO_m(\omega) = S_m(\omega) Rch_{m-t0}(\omega)^*.$$

For a single reflection, the NMO shifts are the  $Rcc_{m-t0}$  lag times. To separate the lags corresponding to different reflectors, we apply a k-means cluster analysis (Kaufman and Rousseuw, 1991). For every cluster, we obtain a unique zero-offset two-way traveltime and velocity of that particular event. The fits in both L1- and L2-norms are evaluated and the one with lowest residuals is selected. This information is then used to obtain a preliminary average velocity model that can be used for migration and/or time-to-depth conversion.

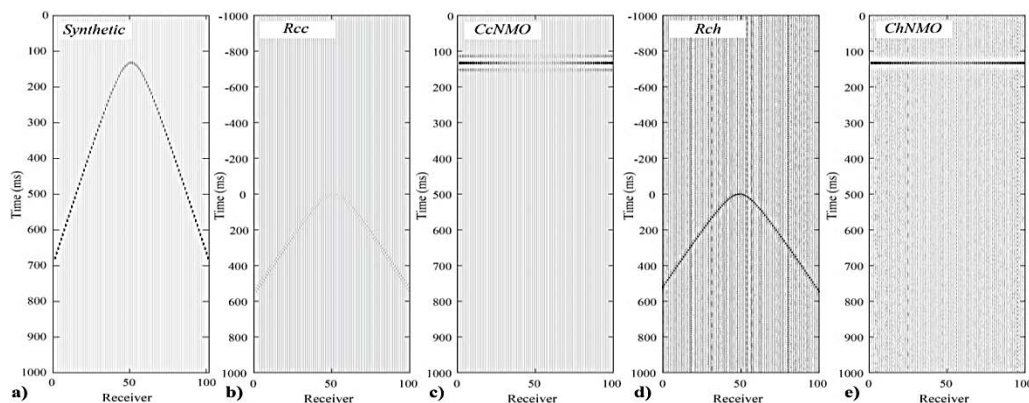
## Case studies

The method was first tested on a synthetic CMP gather with a single reflection originating from an interface at 100 m below the surface separating the top layer (1500 m/s) and the halfspace (3000 m/s). Split-spread geometry with 100 receivers spaced 50 m and a 50 Hz Ricker wavelet was used.

Complemented with cluster analysis, we also did a test on a field dataset acquired at Lilla Edet quick clay landslide site in southwestern Sweden (Salas-Romero et al., 2016). Along the analyzed profile, glacier movements during the glaciation periods have carved a valley in the granitic-granodioritic bedrock. The valley was subsequently filled by glacial sands, tills, along with coarse- and fine-grained gravel, sand, and clays deposited in a shallow littoral environment with a thickness up to 25 – 30 m. The marine-clay layer is of particular importance as these marine clays are prone to liquefaction due to leaching causing landslides, and are known as quick clays in the Nordic countries, Canada, and Alaska (Salas-Romero et al., 2016). The data were acquired in October 2020 with the seismic profile collocated with *Line 1Sa* of Salas-Romero et al. (2016). A 120-unit-long three-component (3C) micro-electro-mechanical (MEMS-based) seismic landstreamer (Brodic et al., 2015) was used to record the data with receiver spacing decreased to 1 m. The entire ca. 240 m profile was acquired by moving the streamer 120 m forward after acquiring all source locations along the first position, without any overlap. An I-beam metal profile stroked laterally with a 7-kg sledgehammer (SV-wave excitation) was used as the source, with two hammer strikes per side to increase SNR. Data were acquired at a sample rate of 1 ms with 3 s record length. We focus on analysis of only the radial component of the 3C landstreamer due to the source nature after vertical stacking of repeated impacts and removal of vertical and transverse components. For all our analyses, we only perform preprocessing by adding a straight CMP line with 0.5 m bin size and apply an automatic gain control (AGC) of 250 ms.

## Results and discussion

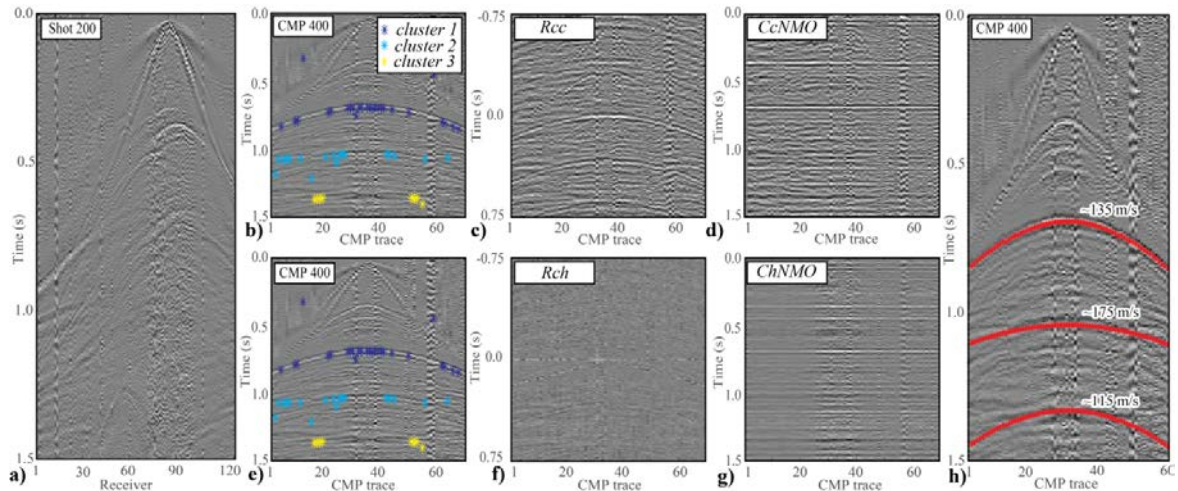
Figure 1a shows the synthetic CMP gather, while Figure 1b-e show the same gather after cross-correlation-based reduction ( $Rcc_{m-t0}$ ), cross-correlation-based NMO corrections ( $CcNMO_m$ ), cross-coherence-based traveltime reduction ( $Rch_{m-t0}$ ), and cross-coherence-based NMO corrections ( $ChNMO_m$ ), respectively. Note that 2% of white noise was added to the cross-coherence results.



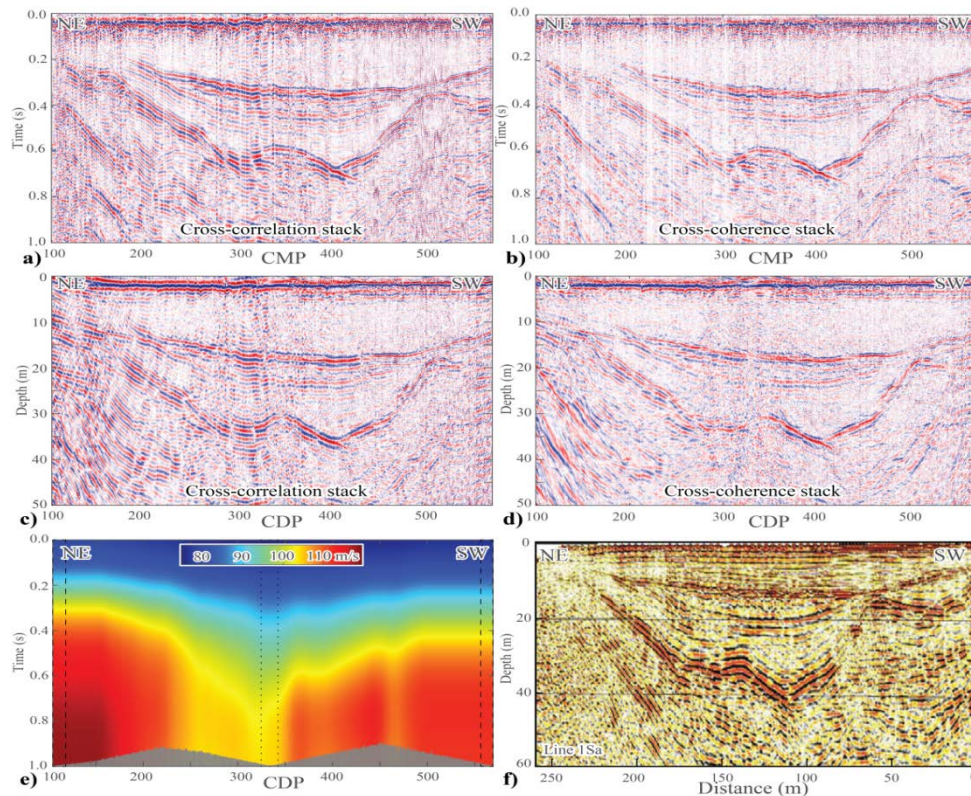
**Figure 1** a) synthetic CMP gather; b) and c) reduced reflection time and NMO-corrected CMP gather after cross-correlation, respectively; d) and e) reduced reflection time and NMO-corrected CMP gather after cross-coherence, respectively. Note the individual time axes and a sharper wavelet of the NMO-corrected reflection after cross-coherence.

Figure 2 shows an example shot gather showing the data quality together with complete application of the method on an example CMP gather with lags and retrieved velocities. In Figure 3 we compare the resulting cross-correlation/cross-coherence sections with the conventional-processing results presented by Salas-Romero et al. (2016). The boxes in Figure 3e indicate locations where the velocities were extrapolated (dashed) or interpolated (dotted) between neighboring CMPs, as the low fold did not allow retrieval of reliable velocity information. Note the sharper wavelets in the cross-coherence (Figure 3b,d) versus cross-correlation (Figures 3a,c) results. Comparison of depth domain migrated sections (Figure 3c,d) versus Salas-Romero et al. (2016) (Figure 3f) shows that the approach is successful in imaging the major reflections at the site. The bedrock appears shallower by ~5%, while other events appear with same depths. The smoothed velocity model obtained (Figure 3e) shows same structure as the time-domain sections (Figure 3a,b) indicating its validity for depth conversion and migration purposes.





**Figure 2** a) Typical quality shot gather; b) example CMP gather (CMP 400), together with retrieved lags after cross-correlation grouped into different clusters as indicated by colors overlaid; c) and d) the same CMP gather after cross-correlation-based reduction (Rcc) and NMO removal (CcNMO), respectively; e) shows same as b), while f) and g) show CMP gather 400 after cross-coherence-based reduction (Rch) and NMO removal (ChNMO), respectively. h) CMP gather 400 with best-fit two-way traveltimes and velocities obtained from cluster analysis calculated for all offsets overlaid and velocities annotated. Note the individual time axes for plots and that only a 250 ms AGC was applied.



**Figure 3** Unmigrated stacked sections obtained without any velocity information via a) cross-correlation- and b) cross-coherence-based NMO removal. c) and d) show depth-converted stacks after frequency-wavenumber migration of a) and b), with 0 m corresponding to ground surface. e) Velocity model obtained via lag cluster analysis smoothed by  $100 \text{ s} \times 50 \text{ CMPs}$  moving average. The grey shaded zone represents CMP fold with max height being fold of 120. Portions within the dashed box were extrapolated while the dotted one interpolated between neighboring CMPs. f) Conventionally processed SH-SH-wave seismic section, modified after Salas-Romero et al. (2016), for comparison purposes. Note that only processing step to obtain the results was a 250 ms AGC.

For the Lilla Edet field data of 30,000 traces, the total algorithm run time – from loading the raw data until producing time-domain stacked sections and the velocity model – was 8-10 min on a standard laptop (16 GB RAM, Core i5 at 2.7 GHz).

## Conclusions

We have applied an automatic, data-driven cross-correlation/cross-coherence based method on CMP gathers to remove the NMO effect without NMO stretch. Comparison of our results with conventional approaches demonstrates the effectiveness of the method. Given that it takes minutes to go from raw field data to a depth converted seismic section, the proposed method show excellent potential for application at other sites and/or for field stack purposes. With site's a priori information about expected velocity bounds, the method also provides a reasonable velocity model that can be used as a base for further improvement or prestack migration.

## Acknowledgements

This study was supported and conducted by the Society of exploration Geophysicists - SEG field camp grant and we are grateful to both SEG and all field camp participants from both Uppsala University and Berlin Technical University for their hard work and motivation.

## References

- Barnes, A.E. [1992] Another look at NMO stretch. *Geophysics*, **57**, 749–751.
- Biondi, E., Stucchi, E. and Mazzotti, A. [2014] Nonstretch normal moveout through iterative partial correction and deconvolution. *Geophysics*, **79**, V131–V141.
- Brodic, B., Malehmir, A., Juhlin, C., Dynesius, L., Bastani, M. and Palm, H. [2015] Multicomponent broadband digital-based seismic landstreamer for near-surface applications. *Journal of Applied Geophysics*, **123**, 227–241.
- Harmankaya, U., Kaslilar, A., Thorbecke, J., Wapenaar, K. and Draganov, D. [2013] Locating near-surface scatterers using non-physical scattered waves resulting from seismic interferometry. *Journal of Applied Geophysics*, **91**, 66–81.
- Kaslilar, A., Harmankaya, U., van Wijk, K., Wapenaar, K. and Draganov, D. [2014] Estimating location of scatterers using seismic interferometry of scattered rayleigh waves. *Near Surface Geophysics*, **12**, 721–730.
- Kaufman, L., and Rousseuw, P. J. [1991] Finding Groups in Data: An Introduction to Cluster Analysis. *John Wiley & Sons, Inc.*
- Liang, S., Hu, T., Qiao, B. and Cui, D. [2022] Reflection Seismic Interferometry via Higher-Order Cumulants to Solve Normal Moveout Stretch. *IEEE Geoscience and Remote Sensing Letters*, **19**, 1–5.
- Perroud, H. and Tygel, M. [2004], Nonstretch NMO. *Geophysics*, **69**, 599–607.
- Place, J., Draganov, D., Malehmir, A., Juhlin, C. and Wijns, C. [2019] Crosscoherence-based interferometry for the retrieval of first arrivals and subsequent tomographic imaging of differential weathering. *Geophysics*, **84**, Q37–Q48.
- Qiao, B., Wang, Q. and Lei, Y. [2021] Correlation-Based Interferometry Method to Enhance Near-Surface Reflection Signals in Surface Active Seismic Exploration. *IEEE Transactions on Geoscience and Remote Sensing*, **59**, 10697–10707.
- Salas-Romero, S., Malehmir, A., Snowball, I., Loughed, B. C. and Hellqvist, M. [2016] Identifying landslide preconditions in Swedish quick clays—insights from integration of surface geophysical, core sample- and downhole property measurements. *Landslides*, **13**, 905–923.
- Sheng, H., Wu, X. and Zhang, B. [2022], Wavelet estimation and nonstretching NMO correction. *Geophysics*, **87**, V193–V203.